



A Case Study: Heavy Rainfall Event Comparison Between Daily Satellite Rainfall Estimation Products with IMD Gridded Rainfall Over Peninsular India During 2015 Winter Monsoon

Anil Kumar Singh¹ · Virendra Singh¹ · K. K. Singh¹ · Jayant Nath Tripathi² · Amit Kumar¹ · Anil Kumar Soni¹ · M. Sateesh¹ · Chinmay Khadke¹

Received: 8 August 2017 / Accepted: 9 January 2018 / Published online: 23 February 2018

© Indian Society of Remote Sensing 2018

Abstract

India Meteorological department (IMD) used INSAT-3D Meteorological Satellite Imager data to drive two type rainfall estimation products viz-Hydro Estimate (HE) and INSAT Multi-Spectral Rainfall Algorithm (MSRA) on half hourly rainfall rate and daily accumulated rainfall in millimeter (mm). Integrated Multi-Satellite Retrieval for GPM (IMERG) product is being derived by NASA and JAXA by using Global Precipitation Mission (GPM) satellites data. MSRA and GPM (IMERG) are gridded data at 10 km spatial resolution and HE is available at pixel level (4 km at Nadir). IMD provides gridded rainfall data at $0.25^\circ \times 0.25^\circ$ resolution which is based on wide coverage of 6955 actual observation. In present study, validation of INSAT-3D based Hydro Estimator (HE), INSAT Multi-Spectral Rainfall Algorithm (MSRA) and Integrated Multi-Satellite Retrieval for GPM (IMERG) of Global Precipitation Mission (GPM) satellites are carried out with IMD gridded data set for heavy rainfall event during winter monsoon, over peninsular India (November–December 2015). In validation, Nash–Sutcliffe efficiencies (NSE), RMSE, Correlation, Skilled scores are calculated at grid level for heavy and very heavy rain categories and the values of NSE of HE ($-32.36, -3.12$), GPM ($-68.67, -2.39$) and MSRA ($-0.02, 0.28$) on 16th November 2015 and HE ($-13.65, -1.69$), GPM ($-43.79, -2.94$) and MSRA ($-1.08, -1.60$) on 2nd Dec 2015, for heavy and very heavy rainfall. On both days, HE is showing better rainfall estimate compare to GPM for Heavy rainfall and GPM showing better estimation for very heavy rainfall events. In all the cases MSRA is underestimating, if daily rain fall exceeded 75 mm.

Keywords INSAT3D · Hydro Estimate · MSRA · Nash–Sutcliffe efficiencies · Skill score · Heavy rainfall

Introduction

India is an agricultural country; the SW monsoon season (JJAS) is the main rainfall season for the almost whole country (except Tamil Nadu which gets rain during NE monsoon season (OND)). The climatology of rainfall received in the winter monsoon is highest in October, November months (Charlotte et al. 2012; Kumar et al. 2004). The prediction of cyclones track and its

precipitation depends on the number of observations and its physics parameterisation (Hariprasad et al. 2014; Sateesh et al. 2017). The importance of real time satellite observations and its initial boundary initialization can give better result rather than the data assimilation (Le Marshall et al. 2000; Leslie et al. 1998; Zhihua et al. 2005).

The success and failure of crops in a large region of the country depend on the rainfall during SW monsoon season as it brings over 60–80% of India's annual rainfall (Prakash et al. 2014). India is the seventh largest country in terms of area in the world, therefore, it is very difficult to maintain a network of manual meteorological observatories. Moreover, the numbers of extreme events such as extremely heavy downpours, cloud bursts, floods etc. have increased in near past and as per the views of experts, they will increase in future as nature will become more random and

✉ Anil Kumar Singh
singhanil854@gmail.com

¹ India Meteorological Department, New Delhi 110003, India

² Department of Earth and Planetary Sciences, University of Allahabad, Allahabad 211002, India

difficult to predict due to global climate change. Therefore, it is the need of the hour to have proper and accurate knowledge of the spatial and temporal distribution of rainfall at finer resolutions. Conventionally rainfall over the ground is measured using rain gauges and radar. Rain gauges offer point measurements and thus they do not represent spatial variability of the precipitation that varies from few meters to several kilometres. The distribution of the rain gauges is far from adequate to present the meaningful variability for the study of various rain-induced events/processes, like flash flood, dam failure, river catchment, etc. On the other hand, radars are the better representative of the aerial rain, but their coverage is limited due to their high cost. The radar measurements often suffer due to poor calibration of radar reflectivity and also of Z-e-Relationship. Apart from that, ground clutter and anomalous propagation also mars its usability. At the time of severe weather conditions, ground based observation network often fail to work. In view of the limitations of the ground measurements, the most convenient means to measure the precipitation over a large area is by using the satellite-based methods (Barrett and Martin 1981). Hydrologists all around the world have developed various algorithms to get rainfall estimates from the meteorological satellites (Arkin et al. 1987; Adler et al. 1993, 2000; Todd et al. 2001; Haile et al. 2010; Joyce et al. 2004, etc.). India has deployed three meteorological satellites namely Kalpana-1, INSAT-3A and INSAT-3D in geostationary orbit. Algorithms are developed for the estimation of rainfall by these Indian satellites (Mishra et al. 2009, 2010) which provide rain estimates at a temporal resolution of half-hourly, daily, monthly and seasonal. The satellites offer frequent uniform coverage over the large area. However, the satellite measurements also suffer from large errors. While VIS/IR methods suffer from their inability to sense hydrometeors directly (Bhandari and Varma 1995), microwave measurements suffer due to their coarser spatial and temporal resolution, rain variability within their large footprint referred as beam filling problem, uncertainty in the drop-size distribution, drop temperature, fall velocity and shape and orientation of the drops etc. (Varma et al. 2003; Gairola et al 2003; Varma and Liu 2006, 2010; Varma and Pal 2012). Due to the inherent inability of IR measurements to directly sense the hydrometeors, the rain retrieval using them is always indirect in nature.

INSAT or the Indian National Satellite System is a series of multipurpose Geostationary satellites launched by ISRO to satisfy the telecommunications, broadcasting, meteorology, and search and rescue needs of India. Commissioned in 1983, INSAT is the largest domestic communication system in the Asia Pacific Region, designed for enhanced meteorological observation and monitoring of land and ocean surfaces of weather forecasting and disaster

warning (www.isro.gov.in). In recent years, INSAT-3D a dedicated meteorological spacecraft of INSAT series satellite was launched in 2013 and located at 82° east in geostationary orbit, an altitude of ~ 35, 786 km. INSAT-3D has four payloads, two meteorological payloads namely: Six channel Imager, Nineteen channels IR Sounder, One Data Relay Transponder and One Satellite Aided Search and Rescue. The INSAT-3D imager provides imaging capability of the earth disc from geostationary altitude in one visible (0.52–0.72 micrometres) and five infrared; 1.55–1.70(SWIR), 3.80–4.00(MIR), 6.50–7.00 (water vapour), 10.2–11.2 (TIR-1) and 11.5–12.5 (TIR-2) bands. The ground resolution at the sub satellite point is nominally 1 km × 1 km for visible and SWIR bands, 4 km × 4 km for one MIR and both TIR bands and 8 km × 8 km for WV band. Two rainfall products viz-Hydro Estimate (HE) and INSAT Multi-Spectral Rainfall Algorithm (IMSRA) on half hourly rainfall rate and daily accumulated rain fall are being derived from INSAT-3D imager payload data operationally. Another operationally available satellite based rain fall product is Integrated Multi-Satellite Retrieval for GPM (IMERG) product, derived by NASA and JAXA by using Global Precipitation Mission (GPM) satellites data. The rapid urbanization and growth of population has put a strain in the Chennai city infrastructure (Krishnamurthy and Desouza 2015). The sewage system is poor to allow free run-off water in the most monsoon season (Gupta and Nair 2011; Joerin et al. 2012). The rainfall occurred in the November 16th and December 2nd are due to the depression formed in the southwest of Bay of Bengal which this leads to a heavy rainfall activity. The weak sewage system is not good take run-off rain water which leads to flooding in Chennai. The uneven structure of urban structure also makes possibilities of floods in the heavy rainfall activity periods (Srinivasan et al. 2013). The classification of heavy rainfall can also found elsewhere in (Goswami et al. 2006; Rajeevan et al. 2008; Bharti et al. 2016; Bharti and Singh 2015; Tawde and Singh 2015; Pattanaik and Rajeevan 2010). In this study all satellite products like GPM (IMERG near real time), INSAT3D (HE, IMSRA) rainfall products are validated with IMD-gridded data (Pai et al. 2014). Skill scores Probability of detection (POD), False alarm rate (FAR), critical success index (CSI) (Mallett and Brennan 1963; Doswell et al. 1990; Schaefer 1990; Stephenson 2000), NSE (Nash and Sutcliffe 1970).

Data Used

HE (Hydro-estimator)

Hydro-estimator (HEM) provides pixel-scale (4 km at nadir), half-hourly precipitation rate measurements over land and oceans (81°S–81°N and 3°–163°E) and daily, Monthly accumulated rainfall also derived. INSAT-3D Imager observations in TIR1, TIR2 and WV channels combined with Numerical Weather Prediction (NWP) forecasts are used to estimate high spatial-temporal resolution rainfall estimates. The HE uses an algorithm based on IR cloud top temperatures, temperature changes and gradients to produce rainfall rate estimates along with NCEP/GFS parameters, and earth elevation model on half hourly basis. The various corrections and adjustments are applied to the estimates product such as parallax correction (satellite viewing angle), available moisture (derived from the model), and orographic correction. Thermodynamic model is used for calculating EL / LNB correction for warm rain. Orographic correction is carried out using wind and elevation model. Dry atmospheric correction is carried out using RH. Rainfall rate is determined at each pixel using different relationships for convective/strati form type of cloud and relationship dynamically calculated for each pixel.

IMSRA (INSAT Multi-Spectral Rainfall Algorithm)

IMSRA/ IMR product provide rainfall estimation at spatial resolution is $0.1^\circ \times 0.1^\circ$ and temporal resolution is half-hourly over spatial domain 30°E to 120°E and 40°S to 40°N by combining variety of techniques (IR and MW) in a single and comprehensive rainfall algorithm by using spatial interpolation method for box averaging. The products are derived using TIR1 and WV channels brightness temperature from INSAT-3D imager. The observations in IR and WV bands are utilized to classify clouds into several categories, such as low-level clouds, thin cirrus, convective and deep convective clouds, etc. (Roca et al. 2002). The most important aspect of this scheme is that it allows delineation of cirrus clouds, which is one of the major sources of error (Barrett and Martin 1981) in IR-based rain algorithms, and helps identify convective and deep convective rain clouds. In this study, daily accumulated rainfall estimate over Indian region is used. INSAT3D rainfall products HE, IMSRA are collected from the India Meteorological Department, satellite division.

GPM (IMERG)

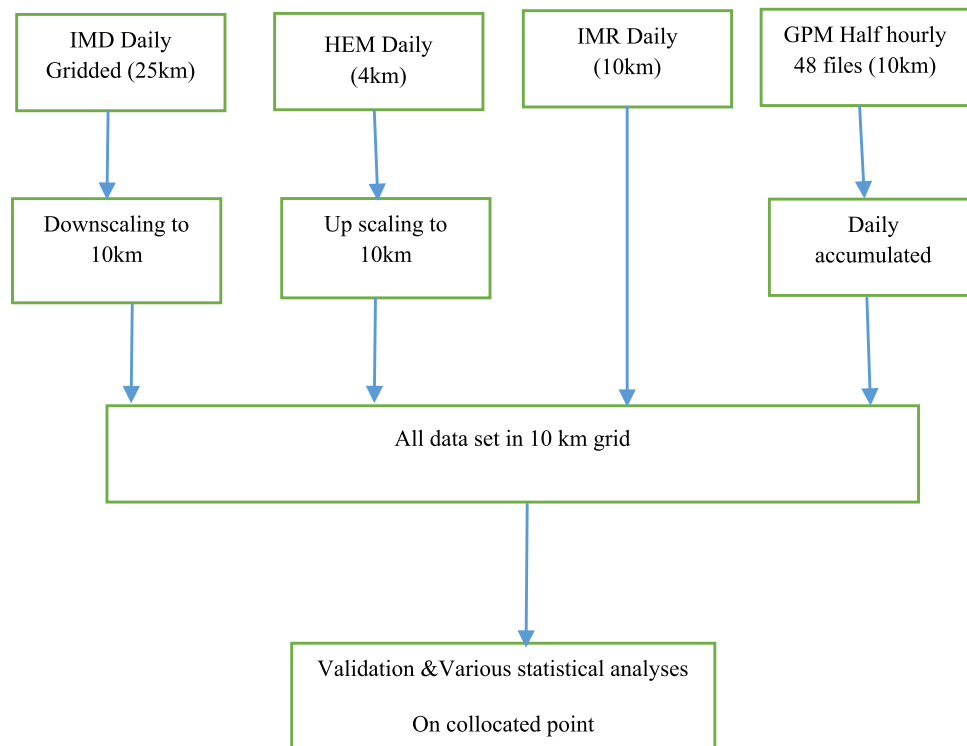
The Global Precipitation Measurement (GPM) mission core satellite was launched in February 2014 with the goal of providing the next-generation, state-of-the-art global quantitative precipitation estimates (QPE). Taking advantage of an international constellation of satellites of opportunity, the Integrated Multi-Satellite Retrievals for GPM (IMERG) produces precipitation estimates in the range 60°N–S at spatial resolution $0.1^\circ \times 0.1^\circ$ on half hour basis. The IMERG precipitation is calibrated to the GPM Microwave Imager/Dual-frequency Precipitation Radar to provide the best possible estimates. IMERG products are produced at three different latencies to accommodate the unique requirements of the various user bases. The “Early” run has a 6-hour latency (for flash flood monitoring, etc.), the “Late” run has a 16-hour latency (for drought monitoring, crop forecasting, etc.) and the “Final” run has a 3-month latency (for research). In this study “Early” run dataset has been used, the data is downloaded via: <https://pmm.nasa.gov/data-access/data-sources>.

IMD Gridded

IMD rainfall gridded dataset is prepared from daily rainfall data of 6955 stations, archived at the National Data Centre, IMD, Pune, by using Shepard method (Pai et al. 2014). Out of these 6955 stations, 537 stations are the IMD observatory stations, 522 stations are under the Hydro-meteorology program and 70 are Agro met stations. Remaining stations are rainfall-reporting stations maintained by state governments.

Methodology

In this study, IMD gridded data (Pai et al. 2014) is used for the validation of various INSAT-3D satellite rain fall derived products such as HEM, IMSRA and GPM satellite derived rainfall products IMERG. To carry out the validation exercise all data need to bring at same spatial resolution and accordingly IMD gridded data is downscaled to 10 km grid from 25 km grid by using bi-linear interpolation method. HEM daily data is up scaled, using pixel averaged method at 10 km grid. IMSRA and GPM (IMERG calibrated data) are available at 10 km grid. The scheme used is depicted as follows.



The satellite rainfall products are validated with IMD rainfall gridded data set and analysis are carried out on the basis of the skill score parameters viz. Probability of Detection (POD), False Alarm Rate (FAR) and Cumulative success Index (CSI), Nash–Sutcliffe efficiencies (NSE), RMSE, Correlation, Percentage of Bias on subdivision wise and category wise (heavy and very heavy rainfall) for rainfall events during winter monsoon, over peninsular India on 16th November 2015 and 2nd December 2015.

Subdivision wise validation statistical analysis parameter of subdivisions Costal Andhra Pradesh, Rayalaseema, Tamilnadu of 16th November and 2nd December 2015 are shown in Tables 1 and 2 respectively. Category wise validation statistical analysis parameter of all grid points of 16 November and 2nd December 2015 are shown in Tables 3 and 4 respectively. Spatial bias map of Costal Andhra Pradesh, Rayalaseema, Tamilnadu sub-divisions for 16 November and 2nd December 2015 are shown in Figs. 1 and 2 and rainfall intensity graph for heavy and very heavy categories is shown in Figs. 3 and 4.

Result and Discussions

Subdivision Wise Analysis

The bias maps between IMD gridded data set and satellite derived rainfall estimate products are plotted for 16th November 2015 and 2nd December 2015 rainfall event as shown in Figs. 1 and 2, respectively. The corresponding skill scores and statistical analysis are shown in Tables 1 and 2 for respective rain events. The analysis shows that when all grid points are considered in all three subdivisions i.e. Costal Andhra Pradesh, Rayalaseema and Tamilnadu then IMSRA has best results in terms of Nash–Sutcliffe efficiencies (NSE), RMSE and Percentage Bias (PBIAS). The values of all these parameters for three subdivisions are NSE (0.65, 0.73, 0.81) RMSE (41.91, 31.71 and 27.19) and PBIAS (37.50, 3.00, 46.80) for 16th November 2016 respectively. Hence at subdivision level for all grid points it can be concluded that the IMSRA estimate is the best match for IMD-gridded rainfall dataset for 16th November 2016. Among HEM and GPM, HEM had performed better in Costal Andhra Pradesh subdivision for which the values are NSE (0.29), RMSE (59.63 mm), PBIAS (43.40%) and R^2 (0.77), whereas GPM had performed better in Rayalaseema (NSE – 2.58, RMSE 114.42 mm, PBIAS 145.30%, and R^2 0.84) and Tamilnadu (NSE – 2.20,

Table 1 16th November 2015 statistical, skill score analysis of GPM, HEM and IMR rainfall with respect to IMD gridded rainfall data

Product	r	R ²	PBIAS (%)	RMSE	NSE	POD	FAR	CSI
Costal Andhra Pradesh total grid point 646								
IMD-GPM	0.84	0.69	132.70	93.26	- 0.74	0.8	0.01	0.80
IMD-HEM	0.88	0.77	43.40	59.63	0.29	0.70	0.02	0.69
IMD-IMR	0.94	0.88	37.50	41.91	0.65	0.99	0.13	0.85
Rayalaseema total grid point 578								
IMD-GPM	0.92	0.84	145.30	114.42	- 2.58	1	0.12	0.87
IMD-HEM	0.89	0.79	175.20	198.70	- 9.79	1	0.12	0.87
IMD-IMR	0.93	0.86	39.00	31.71	0.73	1	0.12	0.87
Tamilnadu total grid point 975								
IMD-GPM	0.95	0.90	169.00	110.55	- 2.20	0.98	0.13	0.85
IMD-HEM	0.90	0.80	197.80	231.55	- 13.04	1	0.14	0.85
IMD-IMR	0.96	0.91	46.80	27.19	0.81	1	0.14	0.85

Table 2 2nd December 2015 statistical, skill score analysis of GPM, HEM and IMR rainfall with respect to IMD gridded rainfall data

Product	r	R ²	PBIAS (%)	RMSE	NSE	POD	FAR	CSI
Costal Andhra Pradesh total grid point 646								
IMD-GPM	0.94	0.89	13.60	20.39	0.85	0.51	0.14	0.47
IMD-HEM	0.76	0.63	- 8.20	33.89	0.57	0.79	0.34	0.56
IMD-IMR	0.89	0.79	- 28.70	33.66	0.58	0.86	0.40	0.54
Rayalaseema total grid point 578								
IMD-GPM	0.97	0.93	- 10.00	16.50	0.87	0.52	0	0.52
IMD-HEM	0.94	0.89	50.40	38.45	0.29	0.59	0	0.59
IMD-IMR	0.88	0.76	- 10.20	26.14	0.67	0.86	0	0.86
Tamilnadu total grid point 975								
IMD-GPM	0.93	0.85	84.90	89.65	- 0.11	0.86	0.11	0.77
IMD-HEM	0.92	0.84	34.50	60.47	0.49	0.95	0.15	0.81
IMD-IMR	0.87	0.74	- 15.80	57.74	0.54	1	0.15	0.84

Table 3 16th Nov 2015 category wise rainfall comparison of GPM, HEM and IMR products with IMD gridded rainfall data

Product	r	R ²	PBIAS (%)	RMSE	NSE
Heavy rain 65.9 to 115.5 (mm) total grid points 29					
IMD-GPM	0.10	0.01	120.10	124.91	- 68.67
IMD-HEM	0.27	0.074	52.90	86.44	- 32.36
IMD-IMR	0.41	0.17	- 5.20	15.12	- 0.02
Very heavy rain 115.6 to 299 (mm) total grid point (54)					
IMD-GPM	0.80	0.64	51.60	101.03	- 2.39
IMD-HEM	0.74	0.55	26.90	111.51	- 3.12
IMD-IMR	0.98	0.95	- 24.30	46.50	0.28

Table 4 2nd Dec 2015 category wise rainfall comparison between IMD and satellite products

Product	r	R ²	PBIAS (%)	RMSE	NSE
Heavy rain 65.9 to 115.5 (mm) total grid points 77					
IMD-GPM	0.42	0.17	78.00	99.06	- 43.79
IMD-HEM	0.46	0.21	32.60	56.66	- 13.65
IMD-IMR	0.42	0.18	- 16.60	21.36	- 1.08
Very heavy rain 115.6 to 376.75 (mm) total grid point (112)					
IMD-GPM	0.70	0.49	45.40	145.87	0.21
IMD-HEM	0.65	0.42	40.50	142.08	- 2.5
IMD-IMR	0.89	0.80	- 55.00	135.89	- 1.40

RMSE 110.55 mm, PBIAS 169% and R² 0.90) subdivisions respectively on 16th November 2016.

On 2nd December 2015, for Costal Andhra Pradesh and Rayalaseema subdivisions GPM has shown better performance compare to other two rainfall products and values are NSE (0.85, 0.87), RMSE (20.39, 16.50) PBIAS (13.60,

- 10.00) however for Tamilnadu subdivision IMSRA perform better and values are NSE (0.54), RMSE (57.74). It is further observed that on 2nd December 2015, the analysis shows an interesting fact that IMSRA had underestimated in all three subdivisions with PBIAS i.e. - 28.70, - 10.20, - 15.80% for Costal Andhra Pradesh,

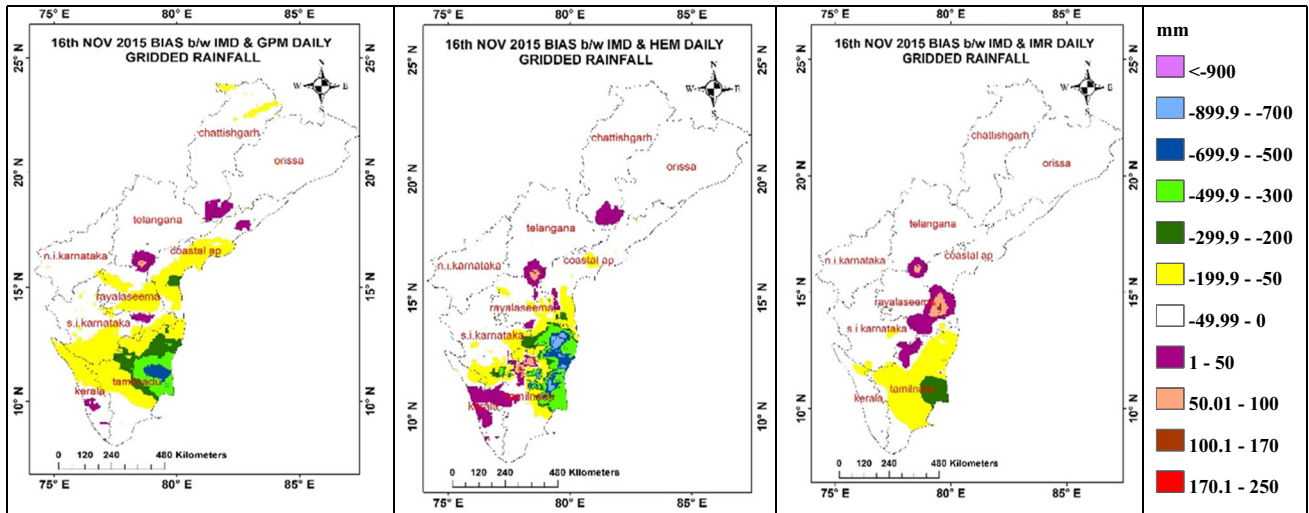


Fig. 1 Bias map between IMD gridded data set and various satellite products (GPM, HEM and IMR from the left to right)

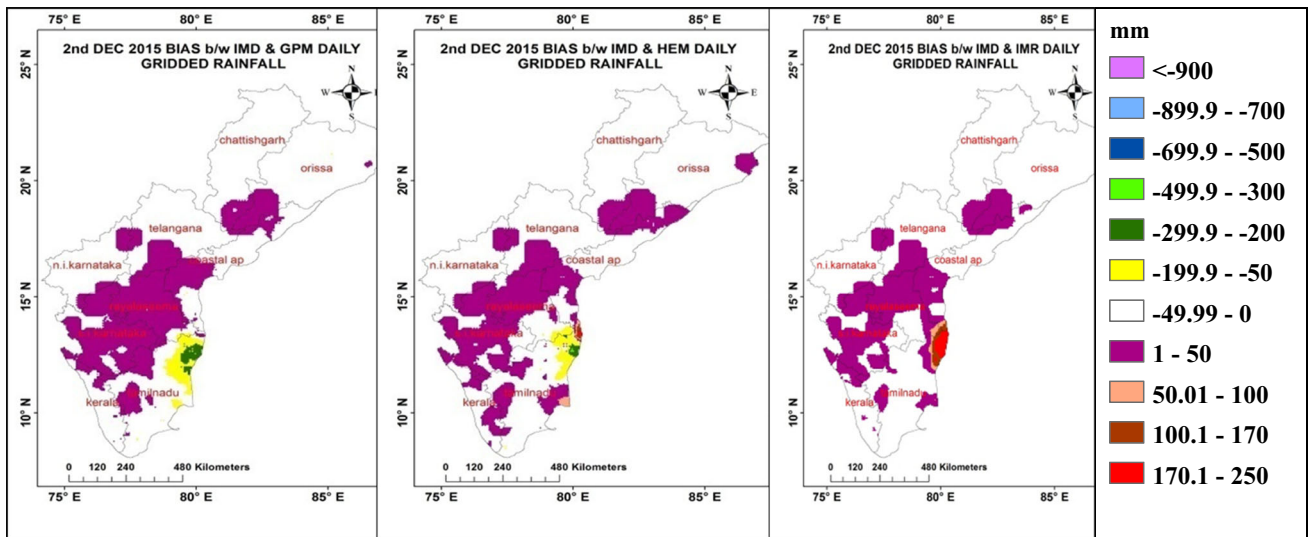


Fig. 2 Bias map of 2nd, Dec-2015 between IMD and various satellite products (GPM, HEM and IMR from the left to right)

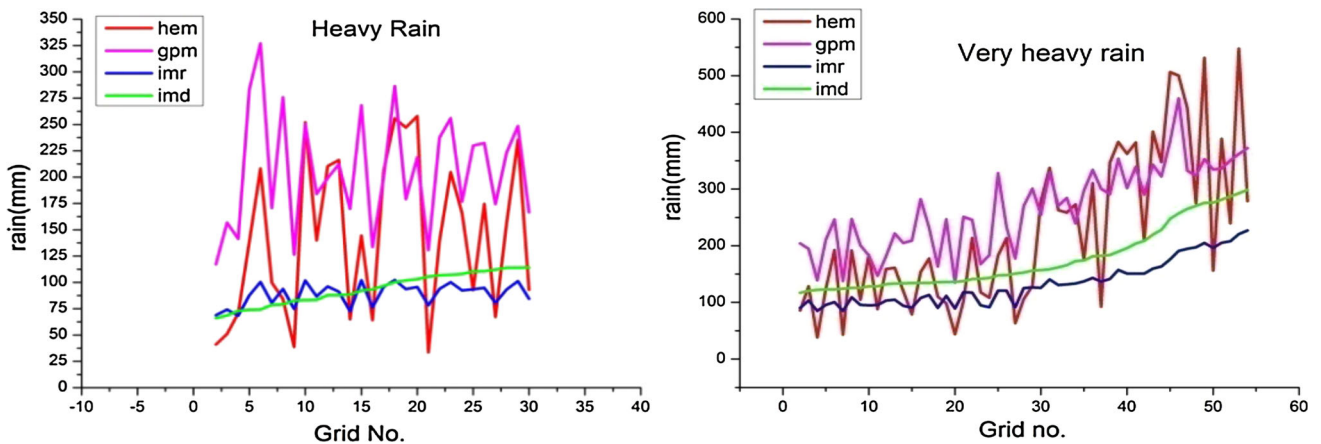


Fig. 3 Rainfall intensity graph on 16th, Nov 2015 between IMD and other satellite products (heavy rain and very heavy rain from left to right)

Royalaseema and Tamilnadu respectively. It can be concluded that IMSRA underestimates during widespread heavy rainfall events (Fig. 2). On 2nd December 2015, HEM has underestimated in Costal Andhra Pradesh subdivision (PBIAS – 8.20%) and GPM had underestimated in Royalaseema subdivision (PBIAS – 10%) respectively. In Tamilnadu subdivision HEM has comparatively performed better with NSE 0.49, RMSE 60.47 mm, PBIAS 34.50%, r 0.92 and R^2 0.84 respectively.

Daily Category Wise Analysis

The intensity plots between IMD gridded data set and satellite derived rainfall estimate products are plotted for respective rainfall event as shown in Figs. 3 and 4 for 16th November 2015 and 2nd December 2015 respectively. The corresponding skill scores and statistical analysis are shown in Tables 3 and 4 for respective rain events. In this analysis only heavy and very-heavy category grid points as per IMD's convention are taken into consideration. The analysis shows that when only heavy and very-heavy category grid points are considered in all three subdivisions i.e. heavy rain 65.9 to 115.5 mm/day (29 grid points), very-heavy rain 115.6 to 299 mm/day (54 grid points) for 16th November 2015, IMSRA has underestimated in both categories with PBIAS – 5.20 and – 24.30% respectively. Similarly, on 2nd December 2015 also, IMSRA has underestimated in both categories with PBIAS – 16.60 and – 55% respectively. From intensity plots it can be seen that IMSRA underestimate when the actual rainfall is above 75 mm/day.

Among GPM and HEM, HEM had performed better in heavy category rain with NSE – 32.36, RMSE 86.44 mm,

PBIAS 52.90%, r 0.27 and R^2 0.074 on 16th November 2015 and NSE – 13.65, RMSE 56.66 mm, PBIAS 32.60%, r 0.21 and R^2 0.21 on 2nd December 2016. Whereas GPM had performed better in very-heavy category rain with NSE – 2.39, RMSE 101.03 mm, PBIAS 51.60%, r 0.80 and R^2 0.64 on 16th November 2016 and NSE 0.21, RMSE 145.87 mm, PBIAS 45.40%, r 0.70 and R^2 0.49 on 2nd December 2015.

Conclusion

In the current study of two heavy rainfall episodes, less bias (32.6%) is reported on December, 2nd with IMD gridded and HE rainfall product. On the basis of daily rainfall analysis carried out category wise, it has been found that in case of very heavy rainfall (greater than 115.6 mm) events GPM (IMERG) performs better than HEM and IMSRA whereas during heavy rainfall (65.6–115.5 mm) events HE performs better than GPM (IMERG) and IMSRA. It is also found that IMSRA performs better than both HEM and GPM (IMERG) up to 75 mm/day rainfall but starts underestimating beyond. Bias during the heavy rainfall events in the post monsoon season are less in the ocean region as compared to the continent. Due to the high resolution and high temporal resolution of HE rainfall product (4 km), it can be used as input for the numerical model to predict the flooding in the urban regions and also to create a merged rainfall product. Further studies will be carried in order to establish the criteria's work out in this study for different seasons and sub divisions.

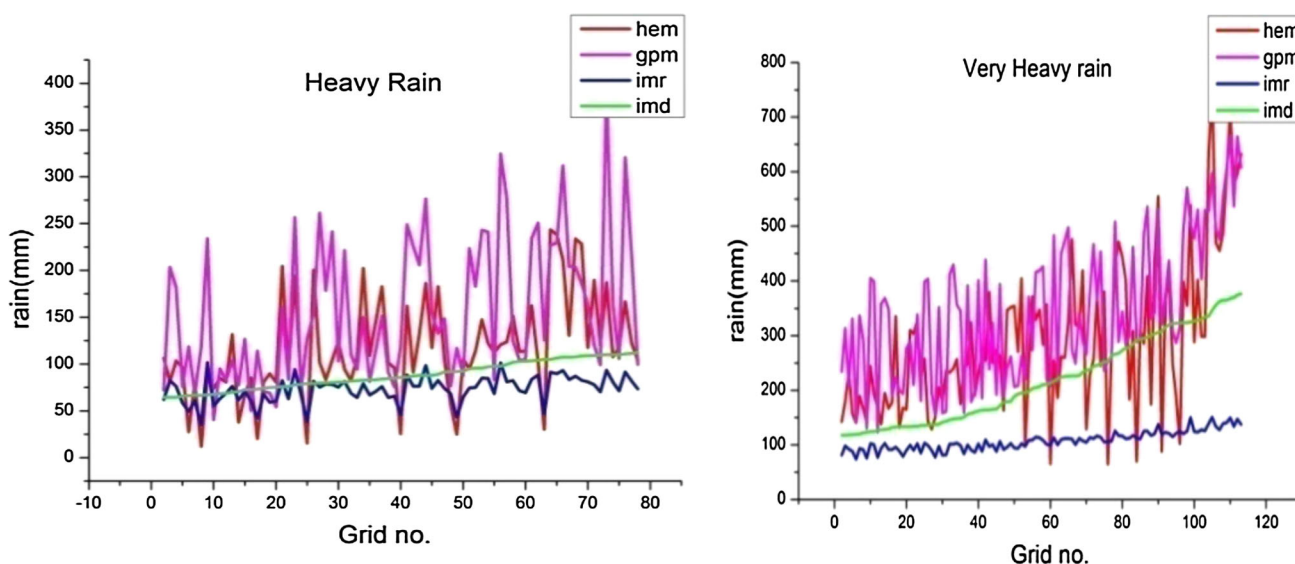


Fig. 4 Rainfall intensity graph on 2nd, Dec 2015 between IMD and other satellite products (heavy rain and very heavy rain from left to right)

Acknowledgements We thankful to DGM of India Meteorological Department for carrying this research work, and We also thankful to Global Precipitation Mission for providing the real time global data.

References

- Adler, R. F., Huffman, G. J., Bolvin, D. T., Curtis, S., & Nelkin, E. J. (2000). Tropical rainfall distributions determined using TRMM combined with other satellite and rain gauge information. *Journal of Applied Meteorology*, 39, 2007–2023.
- Adler, R. F., Negri, A. J., Keehn, P. R., & Hakkarinen, I. M. (1993). Estimation of monthly rainfall over Japan and surrounding waters from a combination of low-orbit microwave and geosynchronous IR data. *Journal of Applied Meteorology*, 32, 335–356.
- Arkin, P. A., & Meisner, B. N. (1987). The Relationship between Large-Scale Convective Rainfall and Cold Cloud over the Western-Hemisphere during 1982–84. *Monthly Weather Review*, 115, 51–74.
- Barrett, E. C., & Martin, D. W. (1981). *The use of satellite data in rainfall monitoring*. London: Academic Press.
- Bhandari, S. M., & Varma, A. K. (1995). Estimation of large scale monthly rainfall over Indian region using minimal INSAT-VHRR data. *International Journal of Remote Sensing*, 16(11), 2023–2030.
- Bharti, V., & Singh, C. (2015). Evaluation of error in TRMM 3B42V7 precipitation estimates over the Himalayan region. *Journal of Geophysical Research: Atmospheres*, 120, 12458–12473. <https://doi.org/10.1002/2015jd023779>.
- Bharti, V., Singh, C., Ettema, J., & Turkington, T. A. R. (2016). spatiotemporal characteristics of extreme rainfall events over the Northwest Himalaya using satellite data. *International Journal of Climatology*, 36, 3949–3962. <https://doi.org/10.1002/joc.4605>.
- Charlotte, B. V., Simon, E. K., George, G., Yesodharan, S., & Ruchith, R. D. (2012). Intra-seasonal oscillation of north east monsoon over southern peninsular India-an investigation. *International Journal of Scientific and Research Publications*, 2, 1–22.
- Doswell, C. A., Davies-Jones, R., & Keller, D. L. (1990). On summary measures of skill in rare event forecasting based on contingency tables. *Weather Forecast*, 5, 576–585.
- Gairola, R. M., Varma, A. K., & Agarwal, Vijay K. (2003). Rainfall estimation using space borne microwave radar and radiometric measurements. *Mausam*, 54(1), 89–106.
- Goswami, B. N., Venugopal, V., Sengupta, D., Madhusoodanan, M. S., & Xavier, P. K. (2006). Increasing trend of extreme rain events over India in a warming environment. *Science*, 314, 1442–1445.
- Gupta, A. K., & Nair, S. S. (2011). Urban floods in Bangalore and Chennai: Risk management challenges and lessons for sustainable urban ecology. *Current Science*, 100, 1638–1645.
- Haile, A. T., Rientjes, T. H., Gieske, A., & Gebremichael, M. (2010). Rainfall estimation at the source of the Blue Nile: A multispectral remote sensing approach. *International Journal of Applied Earth Observation and Geoinformation*, 12, S76–S83. <https://doi.org/10.1016/j.jag.2009.09.001>.
- HariPrasad, K. B. R. R., Srinivas, C. V., Singh, A. B., Vijaya Bhaskara Rao, S., Baskaran, R., & Venkatraman, B. (2014). Numerical simulation and intercomparison of boundary layer structure with different PBL schemes in WRF using experimental observations at a tropical site. *Atmospheric Research*, 145–146, 27–44. <https://doi.org/10.1016/j.atmosres.2014.03.023>.
- Joerin, J., Shaw, R., Takeuchi, Y., & Krishnamurthy, R. (2012). Assessing community resilience to climate-related disasters in Chennai, India. *Journal of Disaster Risk Reduction*, 1, 44–54. <https://doi.org/10.1016/j.ijdrr.2012.05.006>.
- Joyce, R., Janowiak, J. E., Arkin, P. A., & Xie, P. (2004). CMORPH: A method that produces global precipitation estimates from passive microwave and infrared data at high spatial and temporal resolution. *Journal of Hydrometeorology*, 5, 487–503.
- Krishnamurthy, R., & Desouza, K. C. (2015). Chennai, India. *Cities*, 42, 118–129. <https://doi.org/10.1016/j.cities.2014.09.004>.
- Kumar, O. S. R. U. B., Naidu, C. V., Rao, S. R. L., & Rao, B. R. S. (2004). Prediction of southern Indian winter monsoon rainfall from September local upper-air temperatures. *Meteorological Applications*, 199, 189–199. <https://doi.org/10.1017/s1350482704001306>.
- Le Marshall, J., Leslie, L., Morison, R., Pescod, N., Seecamp, R., & Spinoso, C. (2000). Recent developments in the continuous assimilation of satellite wind data for tropical cyclone track forecasting. *Advances in Space Research*, 25, 1077–1080. [https://doi.org/10.1016/s0273-1177\(99\)00445-7](https://doi.org/10.1016/s0273-1177(99)00445-7).
- Leslie, L., LeMarshall, J. F., Morison, R. P., Spinoso, C., Purser, R. J., Pescod, N., et al. (1998). Improved hurricane track forecasting from the continuous assimilation of high quality satellite wind data. *Monthly Weather Review*, 126, 1248–1257.
- Mallett, J. D., & Brennan, L. E. (1963). Cumulative probability of detection for targets approaching a uniformly scanning search radar. *Proceedings of the IRE*, 51, 596–601.
- Mishra, A., Gairola, R. M., Varma, A. K., & Agarwal, V. K. (2009). Study of intense rainfall events over India using Kalpana-IR and TRMM precipitation radar observations. *International Journal of Current Science*, 97, 689–695.
- Mishra, A., Gairola, R. M., Varma, A. K., & Agarwal, V. K. (2010). Remote sensing of precipitation over Indian land and oceanic regions by synergistic use of multi-satellite sensors. *Journal Geophysical Research*, 115, D08106. <https://doi.org/10.1029/2009jd012157>.
- Nash and Sutcliffe. (1970). J.E. Nash, J.V. Sutcliffe River flow forecasting through conceptual models part I—A discussion of principles. *Journal of Hydrology*, 10, 282–290. [https://doi.org/10.1016/0022-1694\(70\)90255-6](https://doi.org/10.1016/0022-1694(70)90255-6).
- Pai, D. S., et al. (2014). Development of a very high spatial resolution (0.250 × 0.250) Long period (1901–2010) daily gridded rainfall data set over the Indian region. *Mausam*, 65(1), 1–18.
- Pattanaik, D. R., & Rajeevan, M. (2010). Variability of extreme rainfall events over India during southwest monsoon season. *Meteorological Applications*, 17(1), 88–104.
- Prakash, S., Sathiyamoorthy, V., Mahesh, C., & Gairola, R. M. (2014). An evaluation of high-resolution multisatellite rainfall products over the Indian monsoon region. *International Journal of Remote Sensing*, 35(9), 3018–3035.
- Rajeevan, M., Bhat, J., & Jaswal, A. K. (2008). Analysis of variability and trends of extreme rainfall events over India using 104 years of gridded daily rainfall data. *Geophysical Research Letters*, 35, L18707. <https://doi.org/10.1029/2008gl035143>.
- Roca, R., Viollier, M., Picon, L., & Desbois, M. (2002). A multi satellite analysis of deep convection and its moist environment over the Indian Ocean during the winter monsoon. *Journal of Geophysical Research*, 107(D19), 8012. <https://doi.org/10.1029/2000JD000040>.
- Sateesh, M., Raju, P. V. S., & Hazards, N. (2017). Numerical simulation of tropical cyclone thane: role of boundary layer and surface drag parameterization schemes. *Natural Hazards*, 20, 11–12. <https://doi.org/10.1007/s11069-017-3020-2>.
- Schaefer, J. T. (1990). The critical success index as an indicator of warning skill. *Weather Forecast*, 5, 570–575.
- Srinivasan, V., Seto, K. C., Emerson, R., & Gorelick, S. M. (2013). The impact of urbanization on water vulnerability: A coupled human–environment system approach for Chennai, India. *Global*

- Environmental Change*, 23, 229–239. <https://doi.org/10.1016/j.gloenvcha.2012.10.002>.
- Stephenson, D. B. (2000). Use of the “odds ratio” for diagnosing forecast skill. *Weather Forecast*, 15, 221–232.
- Tawde, S. A., & Singh, C. (2015). Investigation of orographic features influencing spatial distribution of rainfall over the Western Ghats of India using satellite data. *International Journal of Climatology*, 35, 2280–2293. <https://doi.org/10.1002/joc.4146>.
- Todd, M. C., Kidd, C., Kniveton, D., & Bellerby, T. J. (2001). A combined satellite infrared and passive microwave technique for estimation of small-scale rainfall. *Journal of Atmospheric and Oceanic Technology*, 18, 742–755.
- Varma, Atul K., & Liu, Guosheng. (2006). Small-scale horizontal rain-rate variability observed by satellite. *Monthly Weather Review*, 134(10), 2722–2733.
- Varma, Atul Kumar, & Liu, Guosheng. (2010). on classifying rain types using satellite microwave observations. *Journal of Geophysical Research, Atmospheres*, 115, D7.
- Varma, A. K., & Pal, P. K. (2012). Use of TRMM precipitation radar to address the problem of rain detection in passive microwave measurements. *Indian Journal of Radio & Space Physics*, 41, 411–420.
- Varma, A. K., Pokhrel, S., Gairola, R. M., & Agarwal, V. K. (2003). An empirical algorithm for cloud liquid water from MSMR and its utilization in rain identification. *IEEE Transactions on Geoscience and Remote Sensing*, 41, 1853–1858.
- Zhihua, Z., Yihong, D., Xudong, L., Leiming, M., & Chan, J. C. (2005). The effect of three-dimensional variational data assimilation of QuikSCAT data on the numerical simulation of typhoon track and intensity. *Advances in Atmospheric Sciences*, 22, 534–544.